Sustainable Alginate/PVA/Silica Hydrogel Composites for Efficient Removal and Regeneration in Crystal Violet Adsorption

Andi Nurul Imani Amiruddin, Ahmad Akhib Ainul Yaqin, Dwi Siswanta*, and Agus Kuncaka

Department of Chemistry, Faculty of Mathematics and Natural Sciences, Universitas Gadjah Mada, Sekip Utara, Yogyakarta 55281, Indonesia

Corresponding author:

tel: +62-8157951198
email: dsiswanta@ugm.ac.id

Received: September 16, 2025
Accepted: March 10, 2026

DOI: 10.22146/ijc.111248

Abstract: *The development of reusable and sustainable adsorbents is essential for efficient dye remediation in wastewater treatment. In this study, alginate/polyvinyl alcohol/silica (APS) hydrogel composites were fabricated via a dual-crosslinking strategy using Ca^{2+} and boric acid to enhance structural stability and adsorption performance. Structural integration of the components was confirmed by FTIR and SEM–EDX analyses, revealing strong interactions among alginate, PVA, and silica within a reinforced network. The adsorption behavior toward crystal violet (CV) was systematically evaluated by varying pH, adsorbent dosage, contact time, and initial dye concentration. Under optimal conditions (pH 6, 40 mg adsorbent dosage, 250 mg L^{-1} CV, 120 min adsorption time), the APS composite achieved a maximum experimental adsorption capacity of 143.8 mg g^{-1}. Non-linear kinetic modeling indicated that the pseudo-first-order model provided the best fit (R^2 = 0.993), while equilibrium data were better described by the Langmuir isotherm (R^2 = 0.984), with a predicted monolayer capacity of 169 mg g^{-1}. Mechanistic analysis suggests that CV adsorption is governed by synergistic electrostatic attraction, hydrogen bonding, and partial ion-exchange interactions. Regeneration experiments demonstrated up to 69.7% CV desorption using 0.1 M KCl in ethanol/water, confirming the material's regeneration potential.*

Keywords: *sustainable adsorbent; alginate/PVA/silica; hydrogel composite; crystal violet; regeneration*

■ INTRODUCTION

Synthetic dyes are widely used in industries such as textiles, paper production, cosmetics, and pharmaceuticals, leading to a large volume of colored wastewater [1-2]. Among these dyes, crystal violet (CV), a cationic triphenylmethane compound, has attracted significant interest due to its broad use in textile dyeing, biological staining, and antifungal applications [3]. Despite its usefulness, CV is known to be highly hazardous, exhibiting cytotoxic, genotoxic, and carcinogenic effects on living systems [4]. When released into aquatic environments, CV not only degrades water quality but also threatens human health and disrupts ecosystems [5]. Consequently, the search for efficient and environmentally sustainable methods to eliminate CV from wastewater is of great importance.

Adsorption is considered one of the most effective techniques for dye removal, offering simplicity, high efficiency, and the possibility of adsorbent regeneration [6]. Biopolymer-based hydrogels, particularly alginate, have been widely investigated as eco-friendly adsorbents due to their biodegradability, abundance, and carboxylate groups that favor cationic dye binding [7-8]. Nevertheless, alginate-based hydrogels often exhibit low mechanical strength, limited elasticity, and poor reusability, hindering their practical application in wastewater treatment [9-10].

Polyvinyl alcohol (PVA) is another biocompatible polymer that enhances hydrogel stability and elasticity, but its intrinsic adsorption capacity is relatively low [11]. Incorporation of inorganic materials, such as silica, can improve both structural integrity and adsorption performance due to their high surface area and porosity

[12]. Previous studies have reported alginate–silica or alginate–PVA composites, but the integration of alginate, PVA, and silica into a single hydrogel system remains limited [13-14]. Moreover, most reported composites rely on a single crosslinking agent, which provides insufficient stability for repeated adsorption–desorption cycles.

To address these challenges, this study reports on the synthesis of alginate/PVA/silica (APS) hydrogel composites using double crosslinking with Ca^{2+} and boric acid [15-16]. The APS composite was designed for functional synergy: Alginate provides the primary adsorption sites via its carboxylate groups, PVA improves structural elasticity through covalent boronate linkages [11], and silica acts as a filler to enhance porosity [12]. Among these, alginate is the dominant contributor to dye removal, providing the high negative charge density required for electrostatic binding with crystal violet, while PVA and silica ensure the network's stability and accessibility [9-10].

While alginate-based adsorbents are widely utilized, their practical application is often hindered by poor structural stability and limited adsorption performance in complex aqueous environments. Previous studies reported that the alginate-whey composite exhibited a maximum adsorption capacity of 29 mg g^{-1} for CV [17]. In contrast, another study showed that the maximum monolayer adsorption capacity of CV onto the AM-SA hydrogel was significantly higher at 62.07 mg g^{-1} [18]. This study fills the gap by developing an APS composite using a unique dual-crosslinking strategy (ionic Ca^{2+} and covalent B–O–C). The novelty lies in this synergistic network, which significantly enhances mechanical robustness and reusability compared to conventional materials. The primary scientific contribution is the creation of a stable and regenerable platform specifically optimized for efficient CV removal. The dual crosslinking approach is expected to reinforce mechanical stability while maintaining high adsorption capacity. The composites were systematically evaluated for CV removal under various operational conditions, with particular emphasis on adsorption kinetics, isotherm models, and regeneration efficiency. This work demonstrates that APS hydrogel composites provide a sustainable, efficient, and reusable adsorbent platform for cationic dye remediation in water treatment applications.

■ EXPERIMENTAL SECTION

Materials

All chemicals used were of analytical grade and employed without further purification. Sodium alginate (≥ 95%), PVA (99% hydrolyzed), and silica gel (90–99%) were used as primary components for composite preparation. Glacial acetic acid, calcium chloride ($CaCl_2$, ≥ 97%), boric acid (H_3BO_3, 99%), hydrochloric acid (HCl, 37%), ethanol (≥ 99.9%), and potassium chloride (KCl) were obtained from commercial suppliers. CV dye was used as the model pollutant. Ultrapure water was employed in all experiments.

Instrumentation

The functional groups of the prepared composites were characterized using Fourier transform infrared spectroscopy (FTIR, Shimadzu Prestige-21). The surface morphology, together with the elemental composition, was investigated using scanning electron microscopy (SEM) equipped with energy-dispersive X-ray (EDX) analysis (JEOL JSM-6510LA). In addition, the adsorption experiments were monitored through UV–vis spectrophotometry (Thermo Scientific Orion AquaMate 8100).

Procedure

Synthesis of APS composite

Sodium alginate (1.0 g) and silica gel (1.0 g) were each dissolved in 15 mL of 2% (v/v) acetic acid solution. Separately, PVA (0.5 g) was solubilized in 20 mL of ultrapure water at 90 °C under continuous stirring until fully dissolved. The obtained PVA solution was subsequently mixed with alginate and silica solutions and stirred for 2 h at room temperature. The blended mixture was then added dropwise to a 3% (w/v) $CaCl_2$ solution containing 1% (w/v) H_3BO_3, resulting in the formation of hydrogel beads. The beads were thoroughly rinsed several times with ultrapure water until the pH reached neutrality, followed by drying at 35 °C for 1–2 h prior to further characterization.

Adsorption experiments

The adsorption behavior of the APS composite toward CV was investigated under different experimental parameters. To evaluate the influence of pH, 50 mL of CV solution (100 mg L^{-1}) was adjusted to values between 3 and 8, and then contacted with 20 mg of APS for 2 h. The point of zero charge (pH_{pzc}) was determined by dispersing 20 mg of APS into 0.1 M NaCl solutions at pH 3–8, stirring for 120 min, and measuring the final pH. The effect of adsorbent dosage was evaluated by adding 5–120 mg of APS to 50 mL of 100 mg L^{-1} CV solution at the optimum pH, with a contact time of 120 min. To explore the role of contact time, 40 mg of APS was added to 50 mL of a 100 mg L^{-1} CV solution at the optimum pH, and samples were collected at intervals of 5–180 min. The effect of initial dye concentration was examined using CV solutions at 50–300 mg L^{-1}, under optimal pH and contact time conditions, with 40 mg of APS. Residual CV concentrations in all experiments were quantified using UV–vis spectrophotometry at the maximum absorbance wavelength. All experiments were conducted in triplicate. The reported data represent mean values, with standard deviations (SD) indicated by error bars.

Desorption study

APS composites that had been previously used under optimal adsorption conditions were collected, dried, and subsequently applied for desorption experiments. Each test was carried out in 50 mL of different eluents: 0.1 M HCl, 0.1 M acetic acid, ethanol (60–100%), and KCl (0.1–0.5 M), all prepared in a 1:1 ethanol/water mixture. The suspensions were stirred for 60 min at ambient temperature, after which the concentration of residual CV released into the supernatant was determined using UV–vis spectrophotometry.

■ RESULTS AND DISCUSSION

Characterization

FTIR analysis

Fig. 1 displays the FTIR spectra used to evaluate the functional groups of raw materials and APS composites. The analysis confirms how alginate, PVA, and silica incorporation influences the composite's structural characteristics. A broad absorption band around 3400 cm^{-1} confirmed the presence of hydroxyl (O–H) groups.

During the gelation process, spherical droplets gradually formed an "egg-box" configuration due to selective interactions and crosslinking among the polymer chains, boric acid, and $CaCl_2$ with PVA and sodium alginate. Hydrolyzed boric acid produced borate ions species that reacted with PVA, while the asymmetric COO^- stretching band shifted to 1419 cm^{-1}, indicating the substitution of Na^+ ions with Ca^{2+} in the –COONa groups of alginate. In addition, some of the –COONa groups from the G and M units of alginate were converted into –COOH groups under acidic conditions (Fig. 1(a)) [19-20].

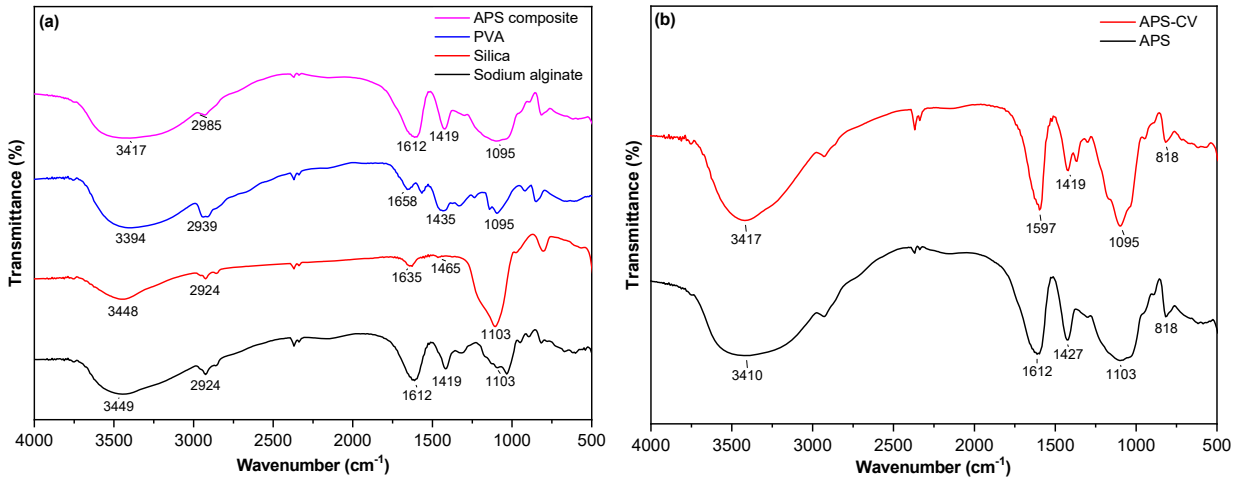

Fig 1. FTIR spectra of (a) raw material APS, (b) APS and APS-CV

The successful formation of the APS hydrogel composite was confirmed by siloxane (Si–O–Si) stretching as illustrated in Fig. 1(b). FTIR spectra revealed the characteristic Si–O–Si stretching shift at approximately 1103 to 1095 cm^{-1}, confirming the successful incorporation of the silica network within the organic polymer. The shift of the carboxylate ($–COO^-$) and O–H stretching bands further indicates the presence of dual crosslinking via ionic interactions with Ca^{2+} and covalent bonding to borate species [15-16].

A dual-crosslinking network governs the enhanced stability of the APS composite. Ionic crosslinking between Ca^{2+} ions and the $–COO^-$ of alginate creates a rigid 'egg-box' structure. Simultaneously, boric acid facilitates covalent crosslinking by forming boronate ester (B–O–C) linkages with the O–H groups of PVA. This combination of ionic and covalent bonding, integrated with the silica matrix, forms a robust interpenetrating network that prevents structural disintegration and ensures high reusability during adsorption-desorption cycles [19-21]. Overall, the FTIR spectra clearly demonstrated structural modifications in the composite before and after dye adsorption. These spectral features provide essential evidence of the active functional groups involved in the binding of CV and highlight the material's potential for use in dye removal and environmental remediation.

SEM-EDX analysis

SEM-EDX spectroscopy was employed to examine the morphology and elemental composition of the APS composite before and after adsorption. Prior to dye uptake, the composite exhibited a relatively smooth, uniform surface, indicating good compatibility among the components within the matrix. After exposure to CV, the surface morphology changed markedly, becoming rougher and more porous as shown in Fig. 2. These alterations indicate that CV molecules were successfully deposited and incorporated into the composite network. The increase in surface irregularities is expected to enlarge the effective surface area available for interaction with dye molecules, thereby enhancing the overall adsorption capacity. Such observations are in line with the main goal of fabricating the composite, namely to achieve greater efficiency in contaminant capture.

EDX analysis provided quantitative elemental composition data for the composite before and after dye adsorption. The carbon content increased from 36.51 to 42.74% after exposure to CV, confirming that the dye molecules contribute additional carbon to the material. This enrichment of carbon indicates that CV molecules are not only attached to the surface but also incorporated into the composite matrix, reinforcing the presence of chemical interactions during adsorption. Alongside carbon, the relative percentages of oxygen (O) and silicon (Si) were also evaluated. The higher O level observed post-adsorption suggests that functional groups on the composite surface bind CV molecules, most likely via electrostatic forces and hydrogen bonding.

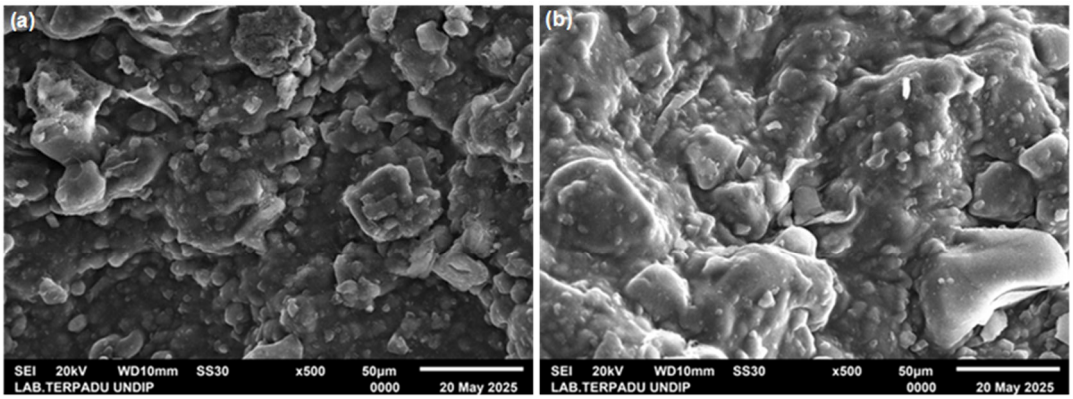

% Mass	C	O	Si	Ca	Na	Al	Total
APS	36.50	53.20	4.67	5.23	0.23	0.17	100
APS-CV	42.40	50.63	3.95	3.02	-	-	100

Fig 2. SEM image of (a) APS and (b) APS-CV

These findings, obtained from SEM-EDX characterization, provide valuable insight into structural and compositional modifications that enhance adsorption, thereby supporting the material's potential use in water treatment applications.

Comparative characterization of APS composite before and after adsorption

Comparative analysis of the APS composite before and after CV adsorption reveals distinct chemical and elemental changes. In the FTIR spectra, the peak corresponding to carboxylate stretching shifted from 1612 to 1597 cm^{-1}, while the O–H intensity decreased, indicating that these groups are the primary sites for electrostatic interaction and hydrogen bonding with the CV molecules. EDX quantitative analysis further supports this: the calcium weight percentage decreased significantly from 5.23 to 3.02% after adsorption. This reduction indicates that Ca^{2+} ions, which initially crosslinked the alginate chains, were partially displaced by the bulky CV cations through an ion-exchange process. The emergence of nitrogen (N) peaks in the post-adsorption spectra further confirms the successful loading of the dye into the porous framework of the APS composite.

Optimization of Experimental Condition

Effect of pH optimum and pH_{pzc}

In adsorption studies, the solution pH is a critical factor because it influences the adsorbent surface charge and governs interactions between charged species. Variations in pH can significantly alter the extent of anion and cation exchange, thereby affecting adsorption efficiency [22]. In this study, the adsorption capacity of the APS composite for CV was examined across a pH range of 3–8. The results showed that the maximum adsorption occurred at pH 6, with a capacity of 192.82 mg g^{-1} (Fig. 3). A steady increase in adsorption was observed from pH 3 to 6, after which a decline was observed at higher pH values. This trend suggests that pH strongly influences the binding behavior of the composite, which is associated with the protonation and deprotonation of silanol groups at the silica surface, as well as electrostatic interactions with the $–COO^-$ groups of alginate [23].

The interaction between the APS composite and CV can be further clarified using the point of zero charge (pzc), determined by the pH-drift method [24]. The pH_{pzc} is the pH at which the adsorbent surface is neutral. For the APS composite, the pH_{pzc} was 5. When the solution pH exceeds this value, deprotonation of surface groups occurs, thereby strengthening the electrostatic attraction between the negatively charged composite surface and the positively charged CV molecules. In contrast, at pH values below the pH_{pzc}, protonation of functional groups causes the composite surface to carry a positive charge, hindering the removal of cationic dyes [18,25]. The pH of the dye solution also affects the ionization state of functional groups on the hydrogel surface, which serve as active adsorption sites. Consequently, selecting an

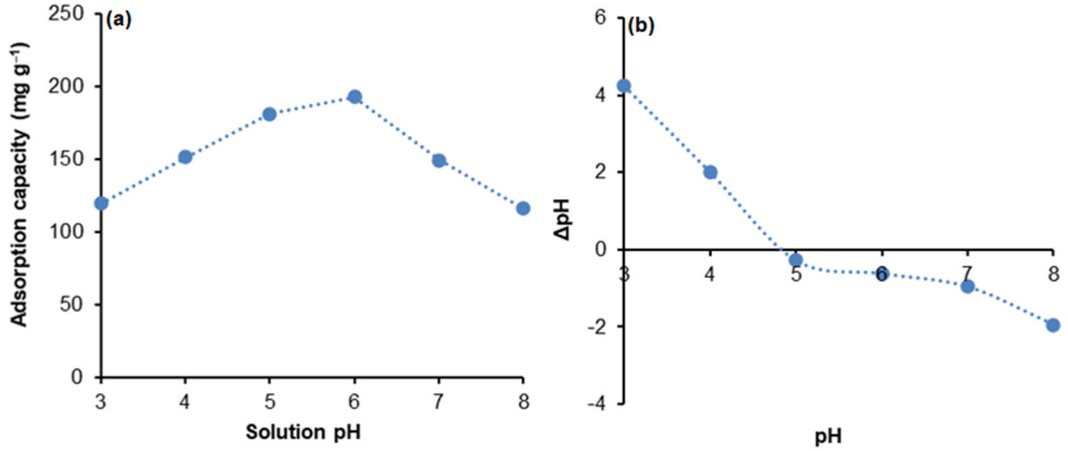

Fig 3. (a) Effect of solution pH on the adsorption capacity of crystal violet (CV) by the APS composite, and (b) determination of the point of zero charge (pH_{pzc}) of the APS composite using 0.1 M NaCl solution

appropriate pH is essential for maximizing electrostatic interactions between the adsorbent and dye ions, ultimately leading to higher adsorption efficiency [7].

Effect of APS dosage

Selecting the appropriate amount of adsorbent is a key factor in adsorption studies, as the adsorbent mass directly influences the efficiency of dye removal from solution [26]. In this work, APS masses ranging from 5 to 100 mg were tested to determine the optimal quantity for CV adsorption. The results showed that adsorption efficiency increased progressively with increasing adsorbent mass, reaching its maximum at around 40 mg (Fig. 4). This improvement can be attributed to the larger surface area and the greater number of active sites available for interaction with dye molecules [17].

Nevertheless, when the APS mass exceeded 40 mg, no substantial enhancement in adsorption was detected. This effect is most likely caused by particle aggregation in the solution, which reduces the accessibility of adsorption sites and weakens the interaction between the dye and the adsorbent [26]. The effect of adsorbent mass on CV removal showed a dual trend. While the removal efficiency increased with higher dosage, the adsorption capacity decreased from 192.82 mg g^{-1} (at 20 mg) to 100.56 mg g^{-1} (at 40 mg). This decline is attributed to the concentration gradient between the dye solution and the adsorbent surface. At lower dosages, each active site is fully utilized due to a high dye-to-adsorbent ratio. Conversely, at higher dosages (40 mg), the abundance of active sites leads to an 'under-saturation' of the adsorbent surface, as the fixed amount of dye molecules is distributed across a greater total surface area. Furthermore, potential aggregation or overlapping of the hydrogel beads at higher dosages may shield some active sites, further contributing to the decrease in q_e [26,29]. Based on these findings, 40 mg was identified as the optimum dose, achieving more than 80% dye removal with an adsorption capacity of 100.56 mg g^{-1} for CV [27]. At this mass, the balance between available surface sites and the effective dye–adsorbent interaction was maximized, ensuring the most efficient adsorption.

Effect of contact time

The influence of contact time on adsorption was investigated using 40 mg of APS composite in a 100 mg L^{-1} CV solution. The adsorption capacity increased rapidly during the early stages of the process, reflecting the abundance of vacant active sites (Fig. 5). After 120 min, the system reached equilibrium with an adsorption capacity of approximately 90 mg g^{-1}, as indicated by the minimal increase in dye uptake beyond this point. This behavior suggests that prolonged contact time leads to saturation of active sites, thereby reducing the potential for further adsorption [28]. Optimizing the contact time is therefore essential to prevent unnecessary energy and resource consumption [29].

To better describe the adsorption dynamics, kinetic models were applied to the experimental data. Both pseudo-first-order (PFO) and pseudo-second-order (PSO) models were tested [17]. The PFO model assumes that the adsorption rate is proportional to the difference

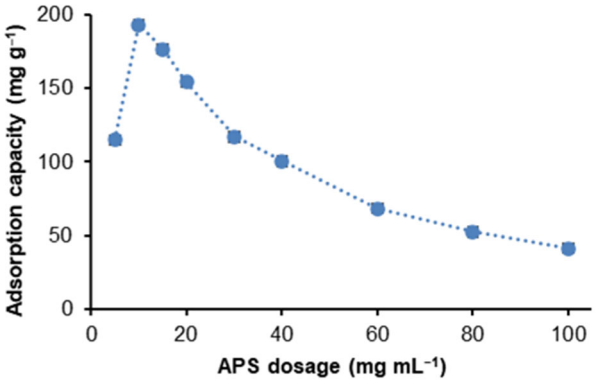

Fig 4. Effect of mass on the adsorption capacity of CV on APS composite

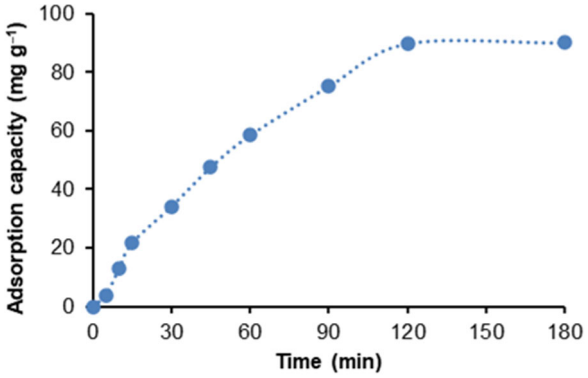

Fig 5. Effect of contact time on the adsorption capacity of CV on APS composite

between the equilibrium and the actual amount adsorbed, reflecting primarily physical interactions. In contrast, the PSO model accounts for the relationships among adsorption rate, adsorbent mass, and contact time, suggesting the involvement of chemical interactions, such as electron sharing or van der Waals forces [17].

To better describe the adsorption dynamics, the experimental data were fitted using non-linear PFO and PSO kinetic models. The non-linear fitting results (Table 1) show that the PFO model provides the best representation of the adsorption kinetics with a higher coefficient of determination (R^2 = 0.993) compared to PSO (R^2 = 0.989). This indicates that the adsorption rate is strongly governed by the availability of accessible sites and the concentration driving force during the early stage, while the system gradually approaches equilibrium after 120 min. Although PSO also provides a good fit, the slightly better performance of PFO suggests that the overall uptake is controlled by a combination of electrostatic interactions and mass-transfer/accessible-site effects rather than solely by chemisorption, as inferred from linear PSO fitting. Therefore, the kinetic behavior of CV adsorption on APS is best described by the PFO model under the investigated conditions.

Effect of concentration on CV solution

Determining the concentration of the dye solution in adsorption studies is crucial, as it directly affects the adsorption capacity and the efficiency of dye removal. In this experiment, the concentration of CV was varied from 0 to 300 mg L^{-1}, and each concentration was tested to determine the maximum amount of dye the APS composite could adsorb. To maintain consistency, all tests were performed under previously optimized conditions: a solution pH of 6, an adsorbent mass of 40 mg, and a contact time of 120 min.

The analysis revealed that the APS composite could adsorb CV with a highest adsorption capacity of 143.75 mg g^{-1} at an optimal concentration of 250 mg L^{-1}. As shown in Fig. 6, at lower concentrations of the cationic dye, the hydrogel nanocomposite particles exhibited numerous active adsorption sites, leading to a high adsorption rate for most dye molecules. However, as the dye concentration increased, the adsorption sites reached saturation, making the adsorption process more challenging due to repulsion between free dye molecules and those already bound to the surface [7]. The slight decrease in q_e at 300 mg L^{-1} compared to 250 mg L^{-1} is attributed to the onset of saturation and minor experimental variability in batch adsorption; however, the overall trend remains consistent with increasing uptake up to the near-saturation region.

Differences in q_e values obtained across optimization experiments are expected because each parameter study was conducted under different initial concentrations and driving-force conditions. Therefore, direct numerical comparison of q_e between separate optimization sets should be interpreted cautiously.

Adsorption isotherms were analyzed to describe the equilibrium relationship between CV and the APS composite. The equilibrium data were fitted using non-linear Langmuir and Freundlich models (Table 2). The Langmuir model produced a better fit (R^2 = 0.99) than the Freundlich model (R^2 = 0.91), suggesting that CV

Table 1. Non-linear kinetic parameters for CV adsorption on APS composite

Kinetic models	Parameters	Value
Experiment	q_e, exp (mg g^{-1})	90.01
Pseudo-first order	$q_{e,1}$ (mg g^{-1})	102
	K_1 (min^{-1})	0.0147
	R^2	0.993
Pseudo-second order	$q_{e,2}$ (mg g^{-1})	142
	K_2 (g mg^{-1} min^{-1})	**8.16×10^{-5}**
	R^2	**0.989**

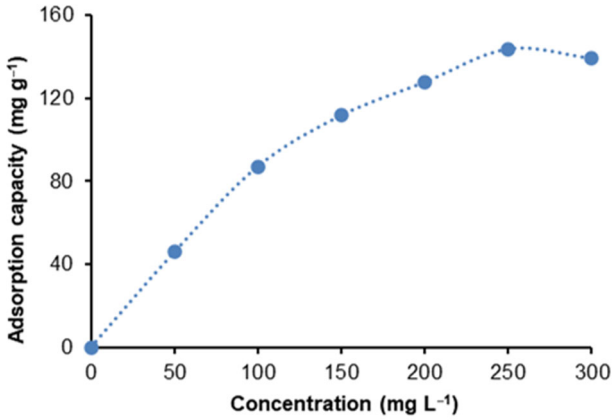

Fig 6. Effect of initial crystal violet (CV) concentration on the adsorption capacity of the APS composite

Table 2. Non-linear adsorption isotherm parameters for CV on APS composite

Isotherm model	Parameter	Value
Langmuir	R^2	0.9900
	q_{max} (mg g^{-1})	169.0000
	K_L (L mg^{-1})	0.0325
Freundlich	R^2	0.9100
	n	2.9300
	K_F (L mg^{-1})	25.5000

adsorption tends to follow monolayer coverage on energetically comparable adsorption sites. The maximum Langmuir adsorption capacity was q_{max} = 168.67 mg g^{-1}, reflecting the high affinity of the APS network toward cationic CV through the availability of –COO^-, –OH, and Si–OH functional groups.

The favorability of adsorption was further evaluated using the Langmuir separation factor (R_L), defined in Eq. (1):

$$R_L = \frac{1}{1 + K_L C_0} \quad (1)$$

where K_L is the Langmuir constant (L mg^{-1}) and C_0 is the initial CV concentration (mg L^{-1}). For the investigated concentration range (50–300 mg L^{-1}), the calculated R_L values fall between 0.381 and 0.093, confirming favorable adsorption of CV onto the APS composite ($0 < R_L < 1$).

Comparison of the maximum adsorption capacities

The comparison of maximum adsorption capacities of various alginate-based hydrogel adsorbents for CV removal (Table 3) shows significant variation. Each adsorbent exhibits different maximum adsorption capacities depending on the experimental conditions; however, the APS composite investigated in this study demonstrated the highest value, reaching 143.75 mg g^{-1}. The main advantage of the APS composite lies in the combination of materials used: SA as the primary component, PVA as a structural reinforcement, silica gel as a filler, and dual crosslinking with $CaCl_2$ and H_3BO_3. This combination provides a porous structure that is more mechanically and thermally stable, as well as an increased surface area. The high maximum adsorption capacity of the APS composite for CV at 250 mg L^{-1} further confirms its effectiveness in removing cationic dyes, particularly CV.

Adsorption Mechanism

FTIR analysis revealed the presence of –OH, –COO^-, and Si–OH groups on the APS composite surface, which act as active binding sites for CV. After adsorption, the –COO^- stretching band shifted from 1612 to 1597 cm^{-1}, accompanied by a reduction in –OH band intensity. These spectral changes indicate the involvement of –COO^- and –OH groups in the adsorption process.

The adsorption behavior can be rationalized by electrostatic interactions driven by the composite's surface charge. The pH_{pzc} of APS was determined to be 5. At the optimal pH (6), the composite surface becomes negatively charged due to the deprotonation of –COOH and Si–OH groups, thereby enhancing electrostatic attraction toward the positively charged CV molecules. This electrostatic driving force plays a dominant role in the adsorption process.

Table 3. Comparison of the maximum adsorption capacities of various alginate-based hydrogel adsorbents for CV removal

Adsorbent	q_{max} (mg g^{-1})	Kinetic model	Isotherm model	Experimental condition and models			Ref.
				pH	m (mg)	C_0 (mg mL^{-1})	
SA/*Cedrus deodara* sawdust	4.80	PSO	Freundlich	12	40	30	[30]
SA/clinoptilolite/Fe_3O_4	16.53	PSO	Langmuir	8	20	10	[31]
SA/CNT	30.00	PSO	Langmuir	6	40	75	[32]
SA/*Sargassum fusiforme*	84.35	PFO	Langmuir	7	25	100	[33]
Alginate/carbon-CTAP (BASSC)	120	PSO	Freundlich	8	20	30	[34]
Alginate/PVA/silica (APS)	143.75	PFO	Langmuir	6	40	250	This work

Note: m = adsorbent mass; t = contact time; C_0 = initial solution concentration

In addition to electrostatic attraction, hydrogen bonding between –OH groups of APS and nitrogen-containing functional groups of CV may further stabilize the adsorbed molecules. Furthermore, the observed decrease in Ca content from EDX analysis suggests partial ion-exchange interactions, where CV^+ species replace Ca^{2+} ions in the alginate network. This ion-exchange contribution supports the composite's strong affinity for cationic dyes.

The Langmuir isotherm provided a good fit to the equilibrium data, suggesting that adsorption predominantly occurs on energetically comparable surface sites with a tendency toward monolayer coverage. However, the kinetic analysis indicated that the PFO model slightly better described the adsorption rate, suggesting that surface accessibility and concentration-driven mass transfer also influence the uptake process. Therefore, the overall adsorption mechanism is best described as a synergistic process involving electrostatic attraction, hydrogen bonding, and partial ion exchange, rather than being attributed solely to a single chemisorption pathway. The proposed adsorption mechanism is illustrated schematically in Fig. 7.

Desorption Study

Desorption studies elucidate the recovery of both adsorbates and adsorbents, as well as the underlying adsorption mechanisms, making it essential to evaluate adsorbent reusability in adsorption-desorption processes. This study (Fig. 8) explored the desorption of the CV dye using several eluents, including CH_3COOH, HCl, KCl, and ethanol, over 2 h. KCl was utilized with ethanol and water (50:50, v/v) as the solvent. The lowest desorption percentage was observed with ethanol at 60, 80, and 100%, indicating that organic solvents do not readily disrupt the interaction between the dye and the APS composite.

In contrast, variations in KCl concentration at 0.1 and 0.5 M showed the highest desorption efficiency, with 0.1 M KCl achieving 69.65%, followed by 0.5 M at 60.62%. The high recovery with 0.1 M KCl in 50% ethanol

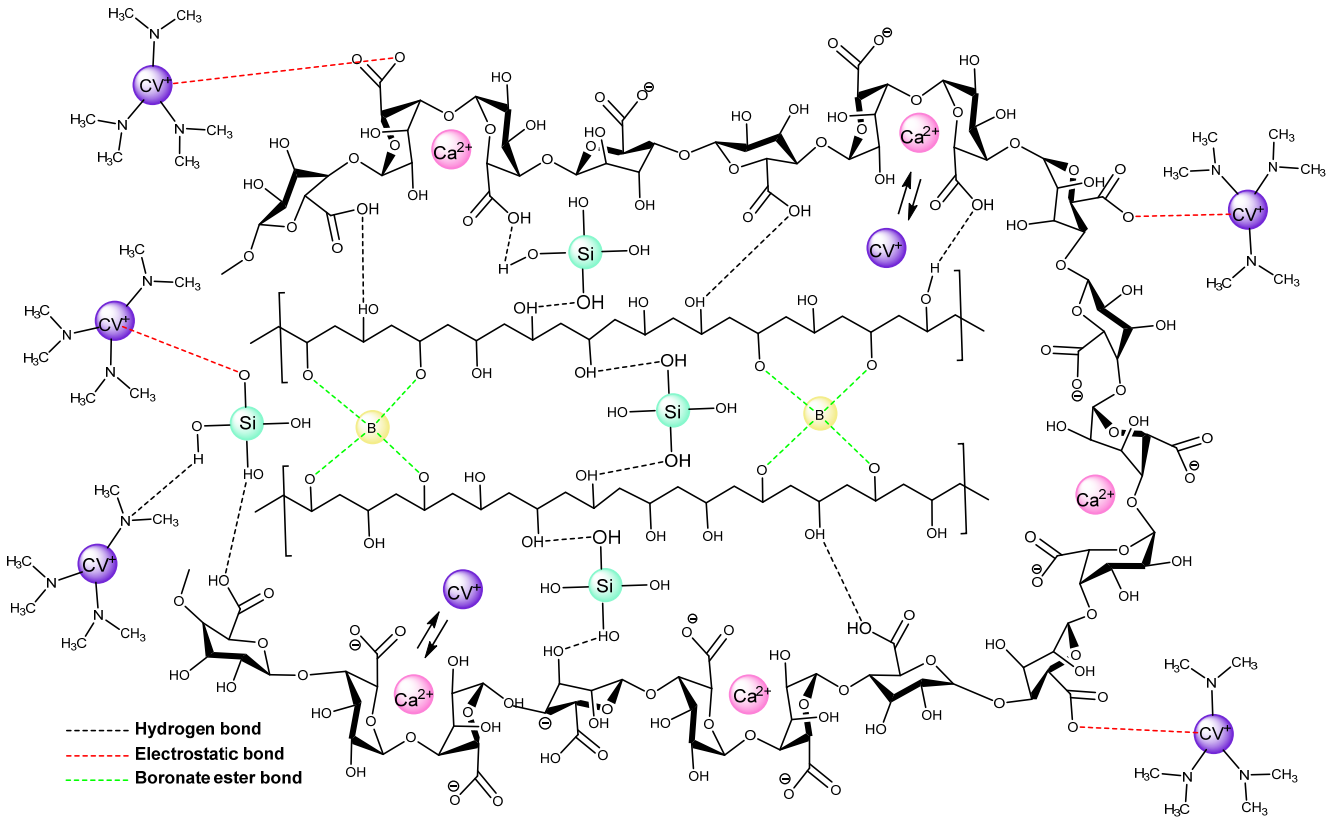

Fig 7. Mechanisms of CV adsorption using APS composite

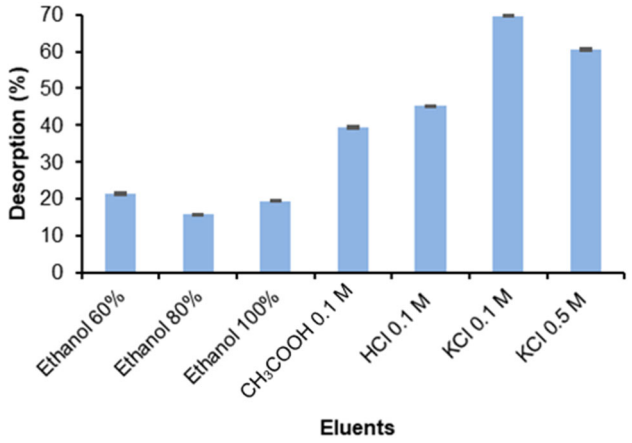

Fig 8. Effect of eluents on CV desorption from APS composite

indicates that an ion-exchange mechanism is dominant, with K^+ ions displacing the CV cations. The 50% ethanol co-solvent maintains matrix integrity by reducing ion activity and water's solvating power. The use of KCl alone in water resulted in structural damage to the APS composite due to the exchange of Ca^{2+} ions, which act as crosslinkers, leading to the solubilization of the adsorbent. The lower efficiency at 0.5 M KCl is likely due to ion shielding, which hinders dye diffusion. This demonstrates that a balance between ionic strength and solvent polarity is crucial for effective regeneration [35].

Desorption efficiency of CV from hydrogel adsorbents in the presence of solvent systems and varying ionic strength, attributing part of the desorption behavior to electrostatic interactions that are screened or competed by ionic species in solution. This supports the notion that increasing ionic strength (e.g., 0.1 M KCl) can weaken electrostatic interactions between the dye and adsorbent and facilitate release [35]. In additional dye-desorption investigations, alcohol-water mixtures are repeatedly employed to balance dye solubility and polymer compatibility, enabling more complete desorption while maintaining hydrogel integrity. The reviewed works show consistent enhancement of desorption efficiency when organic solvents are included, supporting the solvent polarity claim for 0.1 M KCl in 50% ethanol conditions [35-36]. Other specific evidence from alginate-containing hydrogels shows that desorption mechanisms are dominated by weakening of electrostatic binding and by the breakdown of ion–dye networks when environmental conditions or solvent polarity changes, consistent with disruption at the APS interface leading to dye release [36-37].

■ CONCLUSION

Alginate/PVA/silica (APS) hydrogel composites were successfully synthesized via double crosslinking with Ca^{2+} and boric acid, resulting in improved structural stability and adsorption performance. The composites exhibited a maximum adsorption capacity of 143.75 mg g^{-1} for CV under optimal conditions (pH 6, 40 mg adsorbent, 250 mg L^{-1} CV, 120 min). Adsorption followed a PFO kinetic model and was well fit by the Langmuir model, yielding a maximum monolayer capacity of 169 mg g^{-1}, consistent with the high experimental adsorption capacity at 250 mg L^{-1}. Regeneration tests showed that 0.1 M KCl in ethanol/water achieved 70% desorption efficiency, demonstrating the potential reusability of the composites. In summary, this work not only introduces a dual-crosslinked APS hydrogel with enhanced reusability but also provides insight into the adsorption–desorption mechanisms governing cationic dye removal. Overall, APS hydrogel composites represent a sustainable and efficient adsorbent for cationic dye removal and offer promise for practical applications in wastewater treatment.

■ ACKNOWLEDGMENTS

We gratefully acknowledge the support of this work by the Faculty of Mathematics and Natural Sciences, Universitas Gadjah Mada.

■ CONFLICT OF INTEREST

The authors declare that they have no conflict of interest.

■ AUTHOR CONTRIBUTIONS

Andi Nurul Imani Amiruddin conducted the experiments and wrote the manuscript. Dwi Siswanta, Ahmad Akhib Ainul Yaqin and Agus Kuncaka revised the manuscript. All authors agreed to the final version of this manuscript.

■ REFERENCES

[1] Kurosu, M., Mitachi, K., Yang, J., Pershing, E.V., Horowitz, B.D., Wachter, E.A., Lacey, J.W., Ji, Y., and Rodrigues, D.J., 2022, Antibacterial activity of pharmaceutical-grade rose bengal: An application of a synthetic dye in antibacterial therapies, *Molecules*, 27 (1), 322.

[2] Millbern, Z., Trettin, A., Wu, R., Demmler, M., and Vinueza, N.R., 2024, Synthetic dyes: A mass spectrometry approach and applications, *Mass Spectrom. Rev.*, 43 (2), 327–344.

[3] Sun, S., Zhu, Y., Gu, Z., Chu, H., Hu, C., Gao, L., and Zhao, X., 2023, Adsorption of crystal violet on activated bamboo fiber powder from water: Preparation, characterization, kinetics and isotherms, *RSC Adv.*, 13 (9), 6108–6123.

[4] Abdelrahman, E.A., and Basha, M.T., 2025, Facile Synthesis and characterization of $SrCO_3$/MgO/CaO/$CaCO_3$ novel nanocomposite for efficient removal of crystal violet dye from aqueous media, *Inorganics*, 13 (4), 112.

[5] Berradi, M., Hsissou, R., Khudhair, M., Assouag, M., Cherkaoui, O., El Bachiri, A., and El Harfi, A., 2019, Textile finishing dyes and their impact on aquatic environs, *Heliyon*, 5 (11), e02711.

[6] Rashid, R., Shafiq, I., Akhter, P., Iqbal, M.J., and Hussain, M., 2021, A state-of-the-art review on wastewater treatment techniques: the effectiveness of adsorption method, *Environ. Sci. Pollut. Res.*, 28 (8), 9050–9066.

[7] Aljar, M.A.A., Rashdan, S., and Abd El-Fattah, A., 2021, Environmentally friendly polyvinyl alcohol–alginate/bentonite semi-interpenetrating polymer network nanocomposite hydrogel beads as an efficient adsorbent for the removal of methylene blue from aqueous solution, *Polymers*, 13 (22), 4000.

[8] Ling Felicia, W.X., Rovina, K., Supri, S., Matanjun, P., Mohd Amin, S.F., and Abdul Rahman, M.N., 2025, Next-generation sodium alginate hydrogels for heavy metal ion removal: Properties, dynamic adsorption–desorption mechanisms, and sustainable application potential, *Polym. Bull.*, 82 (16), 10587–10637.

[9] Li, X., Li, K., Wu, J., Li, B., Wang, W., and Tang, J., 2024, Facile preparation of sodium alginate gel beads enhanced by polyamino-modified 3D carbon for efficient remediation of organic dyes in wastewater, *Sep. Purif. Technol.*, 339, 126637.

[10] Gheorghita Puscaselu, R., Lobiuc, A., Dimian, M., and Covasa, M., 2020, Alginate: From food industry to biomedical applications and management of metabolic disorders, *Polymers*, 12 (10), 2417.

[11] Ma, Y., Huo, T., Xiao, X., Yin, T., Lei, Y., Zhang, W., Nie, X., and Huang, Q., 2024, Strength modification of sodium alginate–polyvinyl alcohol gel beads and efficient aqueous phase phosphorus removal, *Polym. Bull.*, 81 (8), 7255–7272.

[12] Ransing, A.A., Wang, Q., Dhavale, R.P., Choi, H., Bangi, U.K.H., Parale, V.G., Lee, W., Kanamori, K., and Park, H.H., 2025, Ionotropically-engineered synthesis of mechanically robust hybrid sodium alginate–silica aerogels with enhanced specific surface area for high-capacity and selective dye adsorption from wastewater, *Chem. Eng. J.*, 507, 160590.

[13] Alenezi, H., Gad, E.S., Albassami, N.A., Alatawi, I.S., Alshareef, S.A., Aljowni, M.A., Jame, R., Abdelaziz, M.A., El-din, A.S.B., and Saleh, A.K., 2025, Development of oxidized sodium alginate/silica hybrid as efficient adsorbent for anionic and cationic dyes: Mechanism and thermodynamic studies, *Biomass Convers. Biorefin.*, 15 (12), 18247–18261.

[14] Jin, Q., Diao, X., Fan, Y., Hao, L., Chen, Z., and Guo, Z., 2024, Silica-reinforced AMP-calcium alginate beads for efficient and selective removal of cesium from a strong acidic medium, *ACS Omega*, 9 (29), 32011–32020.

[15] Wang, Y., and Lu, Y., 2023, Sodium alginate-based functional materials toward sustainable applications: Water treatment and energy storage, *Ind. Eng. Chem. Res.*, 62 (29), 11279–11304.

[16] Niewiadomski, K., Szopa, D., Pstrowska, K., Wróbel, P., and Witek-Krowiak, A., 2024, Comparative analysis of crosslinking methods and their impact on the physicochemical properties of SA/PVA hydrogels, *Materials*, 17 (8), 1816.

[17] Djelad, A., Mokhtar, A., Khelifa, A., Bengueddach, A., and Sassi, M., 2019, Alginate-whey an effective and green adsorbent for crystal violet removal: Kinetic, thermodynamic and mechanism studies, *Int. J. Biol. Macromol.*, 139, 944–954.

[18] Pashaei-Fakhri, S., Peighambardoust, S.J., Foroutan, R., Arsalani, N., and Ramavandi, B., 2021, Crystal violet dye sorption over acrylamide/graphene oxide bonded sodium alginate nanocomposite hydrogel, *Chemosphere*, 270, 129419.

[19] Lin, D., Shi, M., Zhang, Y., Wang, D., Cao, J., Yang, J., and Peng, C., 2019, D crateriform and honeycomb polymer capsule with nano re-entrant and screen mesh structures for the removal of Multi-component cationic dyes from water, *Chem. Eng. J.*, 375, 121911.

[20] Yaqin, A.A.A., Suherman, S., Siswanta, D., and Hosseini-Bandegharaei, A., 2025, Fast preconcentration of Pb(II) and Cu(II) in liquid milk by syringe solid-phase extraction using alginate and PVA biopolymer loaded with activated carbon, *Anal. Methods*, 17 (8), 1813–1824.

[21] Braccini, I., and Pe, S., 2001, Molecular basis of Ca^{2+}-induced gelation in alginates and pectins: The egg-box model revisited, *Biomacromolecules*, 2 (4), 1089–1096.

[22] Ogata, F., Sugimura, K., Nagai, N., Saenjum, C., Nishiwaki, K., and Kawasaki, N., 2024, Adsorption efficiency of crystal violet from the aqueous phase onto a carbonaceous material prepared from waste cotton and polyester, *RSC Sustainability*, 2 (1), 179–186.

[23] Fabryanty, R., Valencia, C., Soetaredjo, F.E., Putro, J.N., Santoso, S.P., Kurniawan, A., Ju, Y.H., and Ismadji, S., 2017, Removal of crystal violet dye by adsorption using bentonite – alginate composite, *J. Environ. Chem. Eng.*, 5 (6), 5677–5687.

[24] Kosmulski, M., 2023, The pH dependent surface charging and points of zero charge. X. Update, *Adv. Colloid Interface Sci.*, 319, 102973.

[25] Shi, T., Xie, Z., Mo, X., Feng, Y., Peng, T., and Song, D., 2022, Highly efficient adsorption of heavy metals and cationic dyes by smart functionalized sodium alginate hydrogels, *Gels*, 8 (6), 343.

[26] Jiao, Y., Han, D., Lu, Y., Rong, Y., Fang, L., Liu, Y., and Han, R., 2017, Characterization of pine-sawdust pyrolytic char activated by phosphoric acid through microwave irradiation and adsorption property toward CDNB in batch mode, *Desalin. Water Treat.*, 77, 247–255.

[27] Gong, X.L., Lu, H.Q., Li, K., and Li, W., 2022, Effective adsorption of crystal violet dye on sugarcane bagasse–bentonite/sodium alginate composite aerogel: Characterisation, experiments, and advanced modelling, *Sep. Purif. Technol.*, 286, 120478.

[28] Liu, H., Pan, B., Wang, Q., Niu, Y., Tai, Y., Du, X., and Zhang, K., 2021, Crucial roles of graphene oxide in preparing alginate/nanofibrillated cellulose double network composites hydrogels, *Chemosphere*, 263, 128240.

[29] Li, B., and Yin, H., 2021, Excellent biosorption performance of novel alginate-based hydrogel beads crosslinked by lanthanum(III) for anionic azo-dyes from water, *J. Dispersion Sci. Technol.*, 42 (12), 1830–1842.

[30] Arshad, R., Javed, T., and Thumma, A., 2024, Exploring the efficiency of sodium alginate beads and *Cedrus deodara* sawdust for adsorptive removal of crystal violet dye, *J. Dispersion Sci. Technol.*, 45 (12), 2330–2343.

[31] Noori, M., and Tahmasebpoor, M., 2023, Novel low-cost magnetic clinoptilolite powders/granules for the removal of crystal violet in single and binary systems, *Iran. J. Chem. Chem. Eng.*, 42 (11), 3601–3623.

[32] Oktor, K., Hasirci, G., and Hilmioglu, N., 2025, Preparation and characterization of renewable biopolymer based alginate adsorbent for removing of crystal violet dye from water, *J. Indian Chem. Soc.*, 102 (7), 101766.

[33] Lv, B., Ren, J., Chen, Y., Guo, S., Wu, M., and You, L., 2022, *Sargassum fusiforme* polysaccharide-based hydrogel microspheres enhance crystal violet dye adsorption properties, *Molecules*, 27 (15), 4686.

[34] Venkataraman, S., Viswanathan, V., Thangaiah, S.G., Omine, K., and Mylsamy, P., 2023, Adsorptive

exclusion of crystal violet dye using barium encapsulated alginate/carbon composites: Characterization and adsorption modeling studies, *Environ. Sci. Pollut. Res.*, 30 (48), 106718–106735.

[35] Aichour, A., Djafer Khodja, H., Zaghouane-Boudiaf, H., Iborra, C.V., and Polo, M.S., 2025, Kinetic adsorption studies of methylene blue and crystal violet dyes removal in single and competitive systems using lemon peels/activated carbon/alginate composite, *React. Kinet., Mech. Catal.*, 138 (1), 303–322.

[36] Rani, I., Warkar, S.G., and Kumar, A., 2023, Removal of cationic crystal violet dye using zeolite-embedded carboxymethyl tamarind kernel gum (CMTKG) based hydrogel adsorbents, *ChemistrySelect*, 8 (29), e202301434.

[37] Yao, J., Yang, H., Zuo, D., Xu, J., and Zhang, H., 2022, Facile preparation and adsorption behavior studies of poly(acrylic acid)-based hydrogels reinforced by hydrogen bonds for methylene blue dye, *J. Polym. Environ.*, 31 (2), 552–564.